

# A possibility of high spin hole states in doped $\text{CoO}_2$ layered systems

Krzysztof Rościszewski<sup>1</sup> and Andrzej M. Oleś<sup>1,2</sup>

<sup>1</sup> Marian Smoluchowski Institute of Physics, Jagellonian University,  
Reymonta 4, PL-30059 Kraków, Poland

<sup>2</sup> Max-Planck-Institut für Festkörperforschung,  
Heisenbergstrasse 1, D-70569 Stuttgart, Germany

E-mail: krzysztof.rosciszewski@uj.edu.pl; a.m.oles@fkf.mpg.de

**Abstract.** We introduce and investigate an effective five-band model for  $t_{2g}$  and  $e_g$  electrons to describe doped cobalt oxides with  $\text{Co}^{3+}$  and  $\text{Co}^{4+}$  ions in two-dimensional  $\text{CoO}_2$  triangular lattice layers, as in  $\text{Na}_{1-x}\text{CoO}_2$ . The effective Hamiltonian includes anisotropic kinetic energy (due to both direct Co-Co and indirect Co-O-Co hoppings), on-site Coulomb interactions parameterized by intraorbital Hubbard repulsion  $U$  and full Hund's exchange tensor, crystal-field terms and Jahn-Teller static distortions. We study it using correlated wave functions on  $6 \times 6$  clusters with periodic boundary conditions. The computations indicate low  $S = 0$  spin to high  $S = 2$  spin abrupt transition in the undoped systems when increasing strength of the crystal field, while intermediate  $S = 1$  spins are not found. Surprisingly, for the investigated realistic Hamiltonian parameters describing low spin states in  $\text{CoO}_2$  planes, doping generates high  $S = \frac{5}{2}$  spins at  $\text{Co}^{4+}$  ions that are pairwise bound into singlets, seen here as pairs of up and down spins. It is found that such singlet pairs self-organize at higher doping into lines of spins with coexisting antiferromagnetic and ferromagnetic bonds, forming stripe-like structures. The ground states are insulating within the investigated range of doping because computed HOMO-LUMO gaps are never small enough.

*Published in: J. Phys.: Condensed Matter* **25**, 345601 (2013) [IOP Select].

PACS numbers: 75.25.Dk, 75.10.Lp, 75.47.Lx

Submitted to: *J. Phys.: Condens. Matter*

## 1. Introduction

Cobalt oxides are quite unique due to large splitting between  $t_{2g}$  and  $e_g$  states in their electronic structure and a nonmagnetic ground state distinguishing  $\text{LaCoO}_3$  from a conventional Mott insulator [1]. In the singlet state ( $S = 0$ ) all  $t_{2g}$  states are filled at each  $\text{Co}^{3+}$  ion, and any magnetic or orbital order is excluded. With increasing temperature this compound undergoes a spin-state transition from a nonmagnetic ( $S = 0$ ) to intermediate spin ( $S = 1$ ) state [2]. In the latter  $t_{2g}^5 e_g^1$  state the orbital  $e_g$  degree of freedom is released and the ordered  $e_g$  orbitals support  $A$ -type antiferromagnetic (AF) order, similar to that observed in  $\text{LaMnO}_3$  [3,4]. This type of order follows in  $\text{LaMnO}_3$  from the spin-orbital model designed for high spin ( $S = 2$ ) states of  $\text{Mn}^{3+}$  ions in  $t_{2g}^3 e_g^1$  configuration [5].

Transitions from low spin to high spin states in other cobalt oxides, including two-dimensional (2D)  $\text{CoO}_2$  triangular lattice layers such as in  $\text{Na}_{1-x}\text{CoO}_2$ , (Bi,Pb)-Sr-Co-O or  $\text{Ca}_3\text{Co}_4\text{O}_9$  compounds, have not been reported so far. The properties of  $\text{Na}_{1-x}\text{CoO}_2$  systems change under doping, with an interesting interplay between the magnetic order and superconductivity [6]. On the one hand, the electronic structure of these systems is of great interest and gives many interesting physical features that follow from intrinsic frustration of magnetic interactions on the triangular lattice. On the other hand, the cobalt ions  $\text{Co}^{3+}$  in the undoped compounds, as for instance in  $\text{NaCoO}_2$ , are nonmagnetic [7] in  $t_{2g}^6$  configuration. This is in contrast to the majority of other cobaltates, with a more conventional three-dimensional (3D) structure, where intermediate or high spin states are found at cobalt ions (of various valence). However, also here doping leads to a radically different behaviour from that of a free charge embedded in a band insulator [8].

Cobaltates with 2D triangular lattice were the subject of intense research [6–15] which led to the common view that nonmagnetic (undoped) parent compounds develop on doping *low spin* symmetric superstructures, some of them ferromagnetic (FM), some of them AF, and some others stripe-like, as described in an excellent paper by Mizokawa [10]. Because in the investigated substances the  $\text{Co}^{3+}$  ions belonging to undoped 2D triangular lattice layers are nonmagnetic which suggests that the  $e_g$  levels are unoccupied in  $t_{2g}^6$  states and stay also unoccupied when doping occurs. In the present paper we are verifying this common view and we provide arguments that the  $e_g$  levels play a prominent role there and could lead to high spin states of  $\text{Co}^{4+}$  ions in some doped systems with triangular lattice. In this respect this paper can be considered as a supplementary to an earlier study of the eleven-band  $d$ - $p$  model in  $\text{Na}_{1-x}\text{CoO}_2$  [15].

The paper is organized as follows. In section 2 we introduce an effective model for 3d electrons and provide available information concerning its parameters. The model is next solved on  $6 \times 6$  clusters for several doping levels by self-consistent calculations based on the Hartree-Fock (HF) approach with electron correlations implemented by an exponential local ansatz, as explained in section 3. The numerical results are presented and analyzed in section 4. The paper is concluded in section 5, where we also point out

certain possible experimental implications of the present studies. Appendix presents the kinetic energy elements for Co-Co hopping in the effective model which includes only  $3d$  orbitals at Co ions.

## 2. The effective model for $3d$ electrons

We investigate strongly correlated electrons in doped 2D monolayer with triangular lattice occupied by  $\text{Co}^{3+}$  ions or  $\text{Co}^{4+}$  ions, such as in  $\text{Na}_{1-x}\text{CoO}_2$  or in (Bi,Pb)-Sr-Co-O compounds. The effective model introduced below takes into account only effective  $d$ -type Wannier orbitals at Co sites (resulting from hybridization of  $3d$  cobalt orbitals with surrounding oxygen  $2p$  orbitals). The hybridization is responsible for renormalisation of the bare cobalt Hamiltonian parameters used below in the effective Hamiltonian. Note that formally one can obtain such an effective Hamiltonian by a procedure of mapping Hartree-Fock or local density approximation with Coulomb interaction  $U$  (LDA+ $U$ ) results, obtained in a multiband model featuring cobalt and oxygen orbitals. Such a mapping should preserve the structure of lowest energy levels.

When the splitting between  $t_{2g}$  and  $e_g$  states is large, it might be argued that a three-band model including  $t_{2g}$  orbitals only could be sufficient to describe the  $\text{Co}^{3+}$  ions in the *low spin* state ( $S = 0$ ) in  $\text{Na}_{1-x}\text{CoO}_2$  or (Bi,Pb)-Sr-Co-O compounds [9–12]. Here we study a five-band model to obtain a better insight into: (i) the effects of doping, i.e., the consequences of introducing  $\text{Co}^{4+}$  ions into the parent (undoped) system with  $\text{Co}^{3+}$  ions; (ii) the crossover regime when due to hypothetical crystal field weakening (and therefore smaller distance between  $t_{2g}$  and  $e_g$  levels) one may expect a transition from low spin to high spin Co ions in the ground state.

The effective Hamiltonian for a 2D triangular lattice of Co ions consists of four parts:

$$\mathcal{H} = H_{\text{kin}} + H_{\text{cr1}} + H_{\text{cr2}} + H_{\text{JT}} + H_{\text{intra}}, \quad (1)$$

The kinetic (hopping) part of the Hamiltonian is:

$$H_{\text{kin}} = \sum_{\{ij\mu\nu\}\sigma} t_{i\mu,j\nu} d_{i\mu\sigma}^\dagger d_{j\nu\sigma}, \quad (2)$$

where  $d_{j\nu\sigma}$  denotes electron annihilation operator at site  $j$ ,  $\nu = xy, yz, zx, x^2 - y^2, 3z^2 - r^2$  labels  $3d$  orbitals, and  $\sigma = \uparrow, \downarrow$  corresponds to up and down electron spin. The nonzero hopping elements describe both indirect cobalt-oxygen-cobalt transitions, and direct cobalt-cobalt hoppings. They are given by two parameters,  $t_0$  and  $t_1$ , and defined in table 1 and table 2 presented in Appendix.

The lattice is characterized by the lattice vectors (we take a lattice constant  $a = 1$ )

$$\mathbf{a}_1 = \frac{1}{\sqrt{2}}(0, 1, -1), \quad \mathbf{a}_2 = \frac{1}{\sqrt{2}}(-1, 0, 1), \quad \mathbf{a}_3 = \frac{1}{\sqrt{2}}(1, -1, 0). \quad (3)$$

These vectors are presented in figure 1 by Indergand *et al* [14]. The parameters of indirect (effective) hoppings  $\propto t_0$  can be obtained from the analysis of a multiband  $d$ - $p$  model — they obey Slater-Koster rules [16] and follow from the lowest order perturbation

theory [17]. For instance, using tight binding formalism we obtain for a  $t_{2g}$  system [13] that the hopping amplitude from  $xy$  orbital at site number 0 via  $p_x$  oxygen orbital to  $zx$  orbital at nearest neighbor site along the lattice vector  $\mathbf{a}_1$  is equal  $t_0 = P_{pd\pi}^2/\Delta$ ; here we use this hopping as a unit and take  $t_0 = 0.3$  eV. More details on the possible choice of the microscopic parameters which justify this value and on finite hopping elements are given in Appendix, see table 1.

The direct cobalt-cobalt hoppings are parametrized by the element  $t_1 \equiv \frac{1}{2}P_{dd\pi}$ , being the hopping between two neighbouring  $t_{2g}$  orbitals lying in the plane perpendicular to the bond direction  $\mathbf{a}_n$  (for instance two  $xy$  orbitals for a bond along  $\mathbf{a}_1$ ); here  $t_1 = 0.05$  eV. All  $d-d$  hopping elements are collected in table 2 in Appendix.

Simplified Jahn-Teller (JT) part of the Hamiltonian was proposed by Toyozawa and Inoue [18] for  $e_g$  and for  $t_{2g}$  deformations:

$$\begin{aligned}
H_{\text{JT}} = & \frac{1}{2} \sum_i \left\{ K_{\text{br}} Q_{1i}^2 + K_{\text{JT}} [Q_{2i}^2 + Q_{3i}^2 + Q_{4i}^2 + Q_{5i}^2 + Q_{6i}^2] \right\} \\
& + g_{\text{JT}} \sum_i \left\{ -Q_{1i} (n_{i,x^2-y^2} + n_{i,3z^2-r^2}) \right. \\
& + Q_{2i} \sum_{\sigma} (d_{i,x^2-y^2,\sigma}^{\dagger} d_{i,3z^2-r^2,\sigma} + d_{i,3z^2-r^2,\sigma}^{\dagger} d_{i,x^2-y^2,\sigma}) + \\
& + Q_{3i} \sum_{\sigma} (d_{i,x^2-y^2,\sigma}^{\dagger} d_{i,x^2-y^2,\sigma} - d_{i,3z^2-r^2,\sigma}^{\dagger} d_{i,3z^2-r^2,\sigma}) + \\
& + Q_{4i} (d_{i,xy,\sigma}^{\dagger} d_{i,zx,\sigma} + d_{i,zx,\sigma}^{\dagger} d_{i,xy,\sigma}) \\
& + Q_{5i} (d_{i,xy,\sigma}^{\dagger} d_{i,yz,\sigma} + d_{i,yz,\sigma}^{\dagger} d_{i,xy,\sigma}) \\
& \left. + Q_{6i} (d_{i,yz,\sigma}^{\dagger} d_{i,zx,\sigma} + d_{i,zx,\sigma}^{\dagger} d_{i,yz,\sigma}) \right\} \quad (4)
\end{aligned}$$

where  $Q_{1i}, \dots, Q_{6i}$  denote static JT deformations of the  $i$ -th  $\text{CoO}_6$  octahedron. To make the model (1) as simple as possible we assume that: (i) the same set of parameters  $\{K_{\text{JT}}, g_{\text{JT}}\}$  is suitable for  $e_g$  ( $Q_{2i}, Q_{3i}$ ) and for  $t_{2g}$  ( $Q_{4i}, Q_{5i}, Q_{6i}$ ) modes, and (ii) the breathing mode  $Q_1$  can be neglected  $K_{\text{br}}/K_{\text{JT}} \gg 1$  (note that in manganites  $K_{\text{br}}/K_{\text{JT}} \approx 2$  [3]). These simplifying assumptions allow one to make only qualitative predictions (concerning the JT effect), but any quantitative analysis would require more precise information about the coupling constants.

In manganites typical values for  $g_{\text{JT}}$  and  $K_{\text{JT}}$  are:  $g_{\text{JT}} = 3.8$  eV  $\text{\AA}^{-1}$  and  $K_{\text{JT}} = 13$  eV  $\text{\AA}^{-2}$ , respectively (see [19] and references therein). For cobalt oxides the values of  $g_{\text{JT}}$  and  $K_{\text{JT}}$  are not known. Here we will arbitrarily assume the same value of  $K_{\text{JT}} = 13$  eV  $\text{\AA}^{-2}$  and we estimate the value of  $g_{\text{JT}} \approx 1.6$  eV  $\text{\AA}^{-1}$  from some experimental data reported in a different cobalt compound. Namely Pradheesh *et al* [20] reported strong  $Q_3$  JT distortion in  $\text{CoO}_6$  octahedra, i.e., two long Co-O (apical) bonds and four shorter Co-O bonds when the central cobalt was  $\text{Co}^{3+}$  ion with an intermediate spin. From their data ( $Q_3 \approx 0.12$   $\text{\AA}$ ) we make a jump to our (different) systems and the crude estimate follows  $g_{\text{JT}} \approx 1.6$  eV  $\text{\AA}^{-1}$ , i.e., the value by half smaller than the one in manganites.

Crystal field part of the Hamiltonian consists of two parts,  $H_{\text{cr1}}$  and  $H_{\text{cr1}}$ . The first

one is responsible for the splitting within the group of  $t_{2g}$  levels,

$$H_{\text{cr1}} \propto \frac{1}{3} \sum_i \left( d_{i,xy,\sigma}^\dagger + d_{i,yz,\sigma}^\dagger + d_{i,zx,\sigma} \right) \left( d_{i,xy,\sigma} + d_{i,yz,\sigma} + d_{i,zx,\sigma} \right). \quad (5)$$

Namely, the orbital  $(|xy\rangle + |yz\rangle + |zx\rangle)/\sqrt{3}$  is placed below two degenerate states:  $\left( |xy\rangle + e^{\pm \frac{2\pi i}{3}} |yz\rangle + e^{\pm \frac{4\pi i}{3}} |zx\rangle \right) / \sqrt{3}$ . According to Bourgeois *et al* [11],  $H_{\text{cr1}}$  can be reexpressed in the form

$$H_{\text{cr1}} = -D_1 \sum_i \sum_{\alpha \neq \beta} d_{i\alpha,\sigma}^\dagger d_{i\beta,\sigma}, \quad (6)$$

where the summation  $\sum_{\alpha \neq \beta}$  runs only over  $\{xy, yz, zx\}$  orbitals. The magnitude of splitting amounts to  $3D_1 \simeq 0.315$  eV, following the results of *ab initio* cluster computations performed for Na<sub>1-x</sub>CoO<sub>2</sub> compounds and other available estimates [11, 21, 22]. We believe that this part of Hamiltonian does not influence the results of the present investigation in any significant way — anyway we include it to be consistent with other models used in this field.

The second (simplified) part of crystal field Hamiltonian modeling depends on the splitting between  $t_{2g}$  and  $e_g$  orbitals and can be expressed using site occupations operators  $n_{i\alpha} = \sum_\sigma d_{i,\alpha,\sigma}^\dagger d_{i,\alpha,\sigma}$  as follows

$$H_{\text{cr2}} = D_2 \sum_i (n_{i,x^2-y^2} + n_{i,3z^2-r^2} - n_{i,xy} - n_{i,yz} - n_{i,zx}), \quad (7)$$

where the (experimental) magnitude of the splitting is large for low spin cobaltates. The following values were suggested: 2.5 eV [13], 1.7 eV [23] and 1.5 eV [24]. In addition, the experimental splitting is strongly dependent on doping [12, 25]. For other kind of cobalt oxides (i.e., not the ones studied in the present paper) Merz *et al* [26] claim that crossover between low spin cobalt ( $S = 0$ ) and intermediate/high spin cobalt oxides occurs at  $\approx 1.0 - 1.4$  eV. How these estimates are related to the model Hamiltonian value of  $D_2$  is difficult to say. The naive estimation (when taking into account only  $H_{\text{cr2}}$  and  $H_{\text{intra}}$ ) is that on-site experimental splitting (between single ion configuration with six  $t_{2g}$  electrons and paramagnetic  $t_{2g}^5 e_g^1$  configuration) is equal  $2D_2 - 5B$  where  $B$  is Racah parameter (see  $H_{\text{intra}}$  below and the following comments). This naive estimate does not take into account correlations and what is more important does not take into account any kinetic effects which arise when including  $H_{\text{kin}}$  and  $H_{\text{cr1}}$  into consideration. Therefore, in this paper, at first  $D_2$  will be treated as a variable parameter but finally we will fix below a representative value of  $D_2 = 1.25$  eV (if we accept  $B = 0.1$  eV then the level splitting is:  $2D_2 - 5B = 2$  eV). Let us stress once again that the energy splitting between  $t_{2g}$  and  $e_g$  levels is a very important parameter. It is large for low spin compounds and small for the ones with intermediate/high spin states [26, 27].

Finally, the third type of splitting which occurs within  $e_g$  levels in the present model is neglected. The paramagnetic ground state in the undoped compound can show some magnetic features upon subsequent doping (due to rising concentration of Co<sup>4+</sup> ions). Let us quote a remark from the literature that for  $g_{\text{JT}} = D_1 = t_1 = 0$  and  $D_2 \gg 1$  the

description of electronic states can be based on a three-band model (with  $t_{2g}$  orbitals  $\{xy, yz, zx\}$  orbitals only) and four kagome sublattices [13,14]. For  $0 \neq D_1 \gg t_0$  we have dispersionless single band model. In reality, however, both  $t_0$  and  $t_1$  play an important role and decide about the electron distribution and total spin in the ground state.

The last part of the Hamiltonian  $H_{\text{int}}$  is strong local on-site electron-electron interaction. Here we adopt a more general form of the degenerate Hubbard model [28,29]

$$H_{\text{int}} = U \sum_{i,\mu} n_{i\mu,\uparrow} n_{i\mu,\downarrow} + \frac{1}{2} \sum_{i,\mu \neq \nu} \left( U - \frac{5}{2} J_{\mu\nu} \right) n_{i\mu} n_{i\nu} - \frac{1}{4} \sum_{i,\mu \neq \nu} J_{\mu\nu} (n_{i\mu,\uparrow} - n_{i\mu,\downarrow})(n_{i\nu,\uparrow} - n_{i\nu,\downarrow}), \quad (8)$$

where  $J_{\mu\nu}$  is the tensor of on-site interorbital exchange elements for  $3d$  orbitals which can be expressed using Racah parameters  $B$  and  $C$  [29,30] (see table 1 given by Horsch [29]). Note that each pair of different orbitals  $\mu \neq \nu$  is included twice in equation (8). In simple situations when the system can be described solely in terms of  $t_{2g}$  orbitals all  $J_{\mu\nu} = 3B + C$  and define the unique Hund's coupling  $J_H$ . Another simple situation is encountered when only  $e_g$  orbitals are partly filled — then all Hund's exchange elements are again the same, and  $J_H \equiv J_{\mu\nu} = 4B + C$ . Cross terms between  $t_{2g}$  orbitals and  $e_g$  orbital are different and smaller (we remind that for  $J_{\mu\nu}$  we take the entries from table 1 in [29]). Furthermore, in the present investigation for the sake of simplicity we use the following empirical ansatz:  $C = 4B$  — in the literature it is frequently used (and is quite realistic [5]) for transition metal oxides with ions in various configurations  $3d^n$ . However, this relation is only approximately satisfied in real compounds and some correlations might be necessary [31].

Some comments are necessary about simplifications we made in equation (8). Namely the last term in equation (8) results from mean field approximation done to original [29] spin-spin  $\text{SU}(2)$  scalar product: the spin symmetry is explicitly broken and the quantization axis is fixed in spin space. Then, the full Hund's exchange interaction is replaced by the Ising term. We neglect here the spin-flip terms in Hund's exchange that go beyond the mean field approximation and could lead to spin-orbital entanglement which could be studied only in more sophisticated many-body treatments [32]. However, this approximation is commonly used, for instance in the  $\text{LDA}+U$  approach, because in the HF approximation (when applied to exact intraatomic interaction) one obtains the same final result for electronic interactions. The second approximation we made here is the neglect of double occupancy transfers occurring due to Coulomb interactions between two different orbitals [28]. The penalty due to these approximations, we have to accept, is twofold: (i) neglect of some contributions when correlations are included, using the HF states, and (ii) this approach excludes explicitly spiral-like spin arrangements; they can not be properly described when using the approximate form of equation (8). These approximations influence quantitatively but not qualitatively the multiplet structure [33]. For a triangular lattice this turns out not to be a serious problem.

The on-site interaction Hamiltonian (8) can be rewritten using the electron density

operators as follows:

$$\begin{aligned}
 H_{\text{int}} = & U \sum_{i,\mu} n_{i\mu,\uparrow} n_{i\mu,\downarrow} + \frac{1}{2} \sum_{i,\mu \neq \nu,\sigma} (U - 3J_{\mu\nu}) n_{i\mu,\sigma} n_{i\nu,\sigma} \\
 & + \frac{1}{2} \sum_{i,\mu \neq \nu,\sigma} (U - 2J_{\mu\nu}) n_{i\mu,\sigma} n_{i\nu,-\sigma}.
 \end{aligned} \tag{9}$$

The estimations of an *average* Hund's exchange  $J_H$  are: 0.84 eV (close to atomic value) [34–36]; 0.72 eV [12] and even a value smaller than 0.7 eV [23]. An effective value of  $J_H = 0.35$  eV deduced from an exact solution of a single CoO<sub>6</sub> cluster which includes strong  $d$ - $p$  hybridization and from fitting to x-ray absorption experiments [9] is much smaller. A small value of  $J_H = 0.28$  eV follows also from *ab initio* computations when exchange interaction is strongly reduced (from the atomic value) by some screening effects [40]. Such values have to be considered as semiempirical parameters while larger values are appropriate when the correlation effects are treated explicitly, as in the present paper. Here we adopt the value following Kroll, Aligia and Sawatzky [9], i.e.,  $J_H = B + 4C \simeq 7B \simeq 0.7$  eV given by  $B = 0.1$  eV.

For Hubbard repulsion  $U$  one finds 5.5-6.5 eV used in multiband HF models by several authors [10, 34, 35]. A much smaller value 2.5 eV (and  $J_H = 0.25$  eV) was used in the eleven-band  $d$ - $p$  model [15] (however this model is different as it includes 3D component — namely the influence of neighbouring Na ions in Na<sub>0.5</sub>CoO<sub>2</sub> on CoO<sub>2</sub> layer). Other values suggested for these systems are: 5.0 eV [36]; 4.5 eV [12] (from fits to XAS experiments) and 4-8 eV used in LDA+ $U$  approaches [23, 37–39]. A much smaller value of 1.86 eV, being renormalised by a factor of three from the atomic value due to strong screening effects (similarly like it happens in cuprates) is reported by Bourgeois *et al* [9]. Quite surprisingly, another reference based on *ab initio* reports  $U \simeq 4.1 - 4.8$  eV [40], i.e., larger values than those one could expect when making comparison with very strong  $J_H$  renormalisation reported in the same paper [40]. Here we adopt a value  $U = 4.5$  eV, i.e., our ratio is  $U/t_0=15$  (it is presumably large enough for a strongly correlated cobalt oxide).

### 3. Computational details

We performed extensive computations for  $6 \times 6$  clusters with periodic boundary conditions (PBC) to establish the ground state at different doping (at zero temperature  $T = 0$ ). Our reference (undoped) state with Co<sup>3+</sup> ions contains  $6 \times 36$  electrons. For each doping, i.e., for fixed number of holes  $n_h$  (number of deficient electrons) we studied separately systems with different numbers of  $n_{h\uparrow}$  — up deficient electrons and  $n_{h\downarrow}$  — down deficient electrons upon constraint  $n_h = n_{h\uparrow} + n_{h\downarrow}$ . For nonmagnetic (or AF) systems with zero total magnetization we have  $n_{h\uparrow} = n_{h\downarrow} = \frac{1}{2}n_h$ . All other possibilities correspond to systems with non-zero total magnetization. Purely FM states have  $n_{h\uparrow} = 0$  and  $n_{h\downarrow} = n_h$ . After long screening of preliminary data we have established that the ground states are unpolarized, with  $n_{h\uparrow} = n_{h\downarrow} = \frac{1}{2}n_h$ .

Coming back to computations, there were two distinct steps made for each parameter set and electron concentration: (i) first, the calculations within the single-determinant HF approximation were performed, and (ii) in the next step the HF wave function was modified to include the electron correlations by employing the local ansatz [41]. This ansatz was successfully applied to several systems, *inter alia* to cuprates [42], nickelates [43], manganites [19] and chemical bonds in molecular systems [44]. Here the HF computations were run starting from each one of many different initial conditions (to get unbiased results we considered up to 10000 nonhomogeneous random charge and spin arrangements for each doping level). In addition, the symmetric patterns known from the literature [10] were also included as possible HF initial conditions and compared with the results obtained for other configurations. For each one of starting initial conditions we obtain on convergence a new HF wave function  $|\Psi_{\text{HF}}\rangle$  which needs to be considered further to implement local Coulomb correlations. Thus, after completing the HF computations we performed correlation computations to obtain the total energy and to identify the optimal ground state configuration. Namely, the HF wave function  $|\Phi_0\rangle$  was modified to include the electron correlation effects by using exponential local ansatz [41],

$$|\Psi\rangle = \exp\left(-\sum_m \eta_m O_m\right)|\Phi_0\rangle, \quad (10)$$

where  $\{O_m\}$  are local correlation operators. The values of variational parameters  $\{\eta_m\}$  are found by minimizing the total energy,

$$E_{\text{tot}} = \frac{\langle\Psi|H|\Psi\rangle}{\langle\Psi|\Psi\rangle}. \quad (11)$$

Here for the local correlation operators we use 25 operators which optimize the density-density correlations,

$$O_m = \sum_i \delta n_{i\mu\uparrow} \delta n_{i\nu\downarrow}, \quad (12)$$

i.e., we use all possible combinations  $\mu, \nu = xy, yz, zx, x^2 - y^2, 3z^2 - r^2$  of orbital indices. The symbol  $\delta$  in  $\delta n_{i\mu\sigma}$  indicates that *only that part* of  $n_{i\mu\sigma}$  operator is included which annihilates one electron in an occupied single particle state belonging to the HF ground state  $|\Phi_0\rangle$ , and creates an electron in one of the virtual empty states. The above local operators  $O_m$  correspond to the subselection of presumably most important electron-pair excitations within the *ab initio* configuration-interaction method (for details see [19] and [43]).

After obtaining the total energy for a given starting condition, we repeat all the procedure from the beginning, i.e., we take the second, third, fourth, ... set of HF initial conditions and repeat all computations to obtain the second, third, fourth, ... , *etcetera*, candidate for a ground state wave function. The resulting set of total energies was inspected and the few lowest ones were identified as probable candidates for the true ground state. At this stage we inspected the resulting charge and spin order (within the set of the selected candidates) and prepared the second much smaller set of initial



HF conditions which on one hand were very similar to our candidates and on the other hand we made small changes to enhance local symmetry according to physical insights. The same procedure of performing HF computations and adding local correlations was repeated and the state with lowest energy was picked as our true ground state. We emphasize that altogether such a procedure is very time and labour consuming but it gives relatively high confidence that, *what we identified as the ground state is indeed realized*, within the present effective model for the considered parameters and doping. We remark that the correlation contributions to the the total energy were found to be important for the correct identification of the ground state (as expected).

#### 4. Numerical results

The first computational scan we performed and presented here is for the ground state in undoped substance for varying crystal-field splitting  $D_2$ , see figure 1. We take a standard set of parameters as described in section 2, which corresponds to a strongly correlated system (all in eV):

$$t_0 = 0.3, \quad t_1 = 0.05, \quad U = 4.5, \quad D_1 = 0.105 \quad (13)$$

and adopt the constraint  $C = 4B$  (the other parameters for the Jahn-Teller terms are given in the caption of figure 1). For a fixed value of Hund's exchange given by  $B = 0.1$  eV and for  $D_2 < 0.87$  eV we found the ground state to be totally charge-homogeneous with AF-like arrangement of high spins (close to  $S = 2$ ) and the electron configuration  $t_{2g}^4 e_g^2$  at each site; in a different systems such high spin states for  $\text{Co}^{3+}$  ions are the subject of current interest [45,46]). After crossing the value of  $D_2 = 0.88$  eV the ground state (again with homogeneous charge distribution) becomes nonmagnetic (with spins  $S = 0$ ) as expected, and the electron configuration is  $t_{2g}^6$ . We performed additional computations within in the range  $0.87 \leq D_2 \leq 0.88$  eV and found that the change of the spin state (and of magnetic order) order occurs abruptly (and it resembles a phase transition). Note that the bulk of computations performed in this paper was done for  $D_2 = 1.25$  eV, i.e., well inside low spin (nonmagnetic) regime for cobalt-oxide compounds. Yet, finite doping generates high magnetic moments, see below.

Knowing that  $\text{Co}^{3+}$  ions in the bulk system are in nonmagnetic  $t_{2g}^6$  configuration, the other computations are done well inside the low spin ( $S = 0$ ) regime. Therefore we have used the fixed value of  $D_2 = 1.25$  eV. In spite of this rather high value of  $D_2$  all the computations clearly show that upon doping localized holes with high spin (close to  $S = 5/2$ ) and with occupied  $e_g$  levels appear as a generic feature of the ground state. This is observed for any doping in the investigated doping range  $0 < x < 1.0$ . We have verified that these high spin states occur in the states characterized by very similar energies per doped hole,

$$E_h = \frac{1}{n_h} \{E_{\text{tot}}(n_h) - E_{\text{tot}}(n_h = 0)\}, \quad (14)$$

where  $n_h$  is the number of holes in the considered  $6 \times 6$  cluster. Energy per one doped hole  $E_h$  increases almost in a linear way with increasing doping level, see figure 2. We

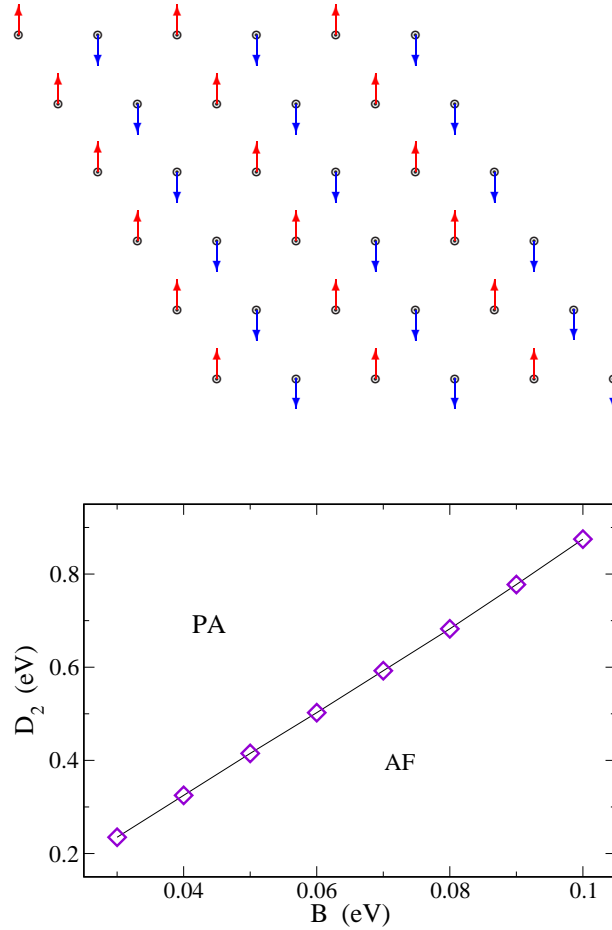


**Figure 1.** *Top panel*— High spin ground state with AF Néel order for zero doping for the triangular lattice obtained on a  $6 \times 6$  cluster with PBC for  $D_2 = 0.87$  eV and  $B = 0.1$  eV. Dots correspond to lattice sites and arrows indicate local high spin states (very close to  $S = 2$ ). Note that at  $D_2 = 0.88$  eV a drastic crossover takes place (for this value of  $B$ ) and all spins collapse to zero when the  $e_g$  states become virtually unoccupied (the electron occupation of each  $e_g$  level is then  $\approx 0.07$ ). *Lower panel*— Phase diagram obtained by varying crystal-field splitting  $D_2$  and Racah parameter  $B$ , for the undoped  $\text{CoO}_2$  triangular plane with  $\text{Co}^{3+}$  ions. AF denotes a region of AF order with high spin ( $S = 2$ ) states of  $\text{Co}^{3+}$  ions, and PA stands for nonmagnetic ground state ( $S = 0$ ) with empty  $e_g$  orbitals. Diamonds are computational results, while the line is a guide for an eye. Other parameters (for both panels) as in equation (13) and:  $g_{\text{JT}} = 1.6 \text{ eV}\text{\AA}^{-1}$ ,  $K_{\text{JT}} = 13 \text{ eV}\text{\AA}^{-2}$ ,  $K_{\text{br}}/K_{\text{JT}} \gg 1$ .

remark that for each doping considered here we did not observe any significant Jahn-Teller static distortions associated with holes (they turn out to be small).

We have not found any interesting local effects in the charge distribution in the dilute limit when the system is doped by  $n_h = 1$  or 2 holes within the  $6 \times 6$  cluster. In these cases the extra charge is distributed almost uniformly over the cluster atoms and all atoms are nonmagnetic. But already for a somewhat higher hole number  $n_h = 4$ , corresponding to low doping  $x = \frac{1}{9}$ , two polaronic states are found, see figure 3(a). At

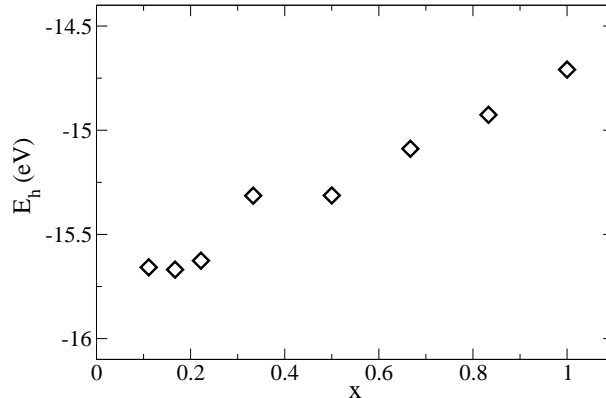


**Figure 2.** Energy  $E_h$  (HF + correlations) per doped hole for increasing doping  $x$  in a  $6 \times 6$  cluster with PBC. For the reference system with no holes (at  $x = 0$ ), the number of electrons is  $6 \times 36$ , the HF energy of the whole cluster is  $E_{\text{HF}} = 1400.538$  eV and the total energy (HF+correlations) is  $E_{\text{tot}} = 1400.002$  eV. Parameters as in equation (13) and:  $B = 0.1$  eV,  $D_2 = 1.25$  eV,  $g_{\text{JT}} = 1.6$  eV $\text{\AA}^{-1}$ ,  $K_{\text{JT}} = 13$  eV $\text{\AA}^{-2}$ ,  $K_{\text{br}}/K_{\text{JT}} \gg 1$ .

each atom of the polaron the electron density is close to 5.2 and a high spin  $S \simeq \frac{5}{2}$  arises. Large spins arise pairwise and are oriented in the opposite way — we suggest that they would give a nonmagnetic singlet state when the quantum spin fluctuations were also included. For this low level of doping the polarons are isolated and no phase separation is found.

For low doping  $x = \frac{1}{6}$  and  $x = \frac{2}{9}$ , see figures 3(b) and 3(c), we observe again high spin states of doped holes, essentially the same spin values  $S \simeq \frac{5}{2}$  as for the case of  $x = \frac{1}{9}$ . The holes with low or intermediate spin values are absent in all cases (but they are found in metastable states, i.e., for local HF minima with higher energies). One finds tendency to form locally bound singlet states, i.e., up-spin and down-spin pairs with both spins placed close to each other. For  $x = \frac{1}{6}$  the stripe-like one-dimensional (1D) structure (in each sixth line with AF order) is clearly emerging, see figure 3(c). This is a precursor state of the ordered 1D structures which occur at higher hole doping, see below.

At this place we would like to make a somewhat obvious but still very important observation that the doping level in the cluster  $x$ , i.e., the number of deficient electrons per site ( $x = n_h/N$ , where  $N = 36$ ) and the subscript  $x$ , say in the chemical formula  $\text{Na}_{1-x}\text{CoO}_2$ , are not the same. For low doping levels in various transition metal oxides they may turn out to be approximately the same but there is no such guarantee for cobaltates. The well known example are  $\text{YBa}_2\text{Cu}_3\text{O}_{6+x}$  superconductors, where the actual hole concentration  $x$  is quite distinct from the chemical doping [47]. One should keep this observation in mind when trying to compare any computational results reported here with the experimental data for particular cobalt oxides.

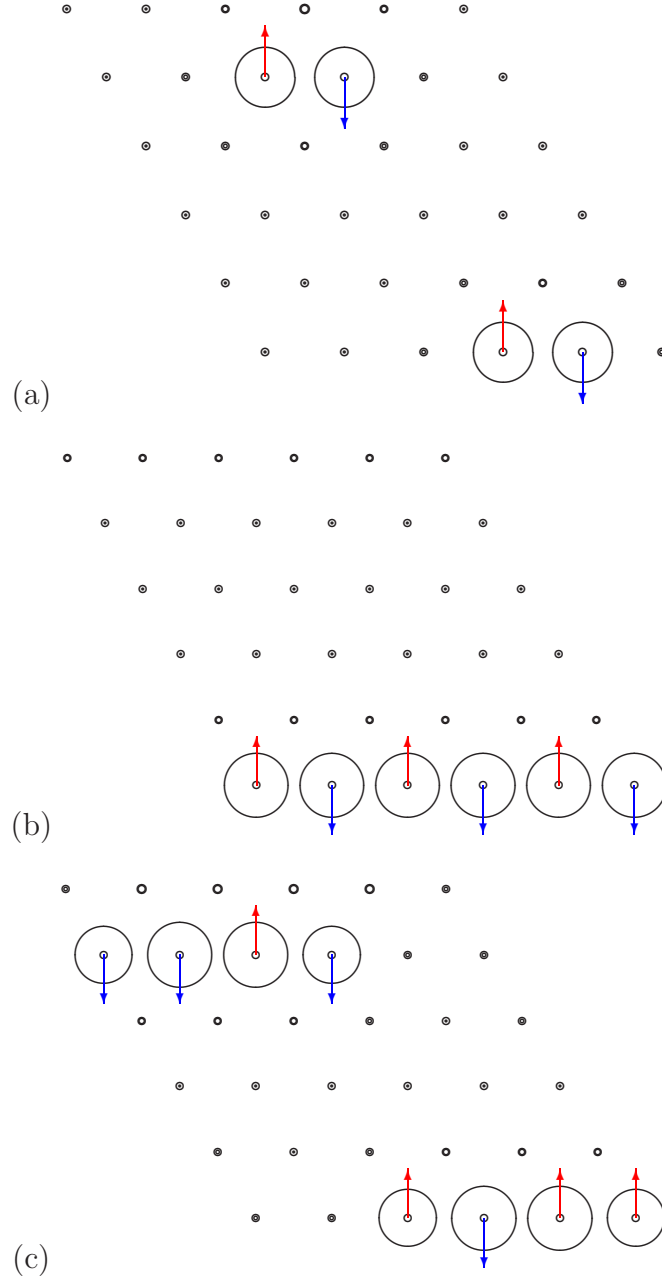


**Figure 3.** High spin states at doped holes (spin values very close to  $S = \frac{5}{2}$ ) in ground states obtained in the lowdoping regime: (a)  $x = \frac{1}{9}$  (4 doped holes, upper panel), (b)  $x = \frac{1}{6}$  (6 doped holes, middle panel), and (c)  $x = \frac{2}{9}$  (8 doped holes, lower panel). Dots correspond to lattice sites and arrows indicate high spin states. Circle are corresponds to hole charges (each big circle denotes a hole with  $\sim 0.8e$  missing). Parameters as in equation (13) and:  $B = 0.1$  eV,  $D_2 = 1.25$  eV,  $g_{\text{JT}} = 1.6$  eV $\text{\AA}^{-1}$ ,  $K_{\text{JT}} = 13$  eV $\text{\AA}^{-2}$ ,  $K_{\text{br}}/K_{\text{JT}} \gg 1$ ; we remind that the  $t_{2g} - e_g$  splitting is well inside low spin regime of an undoped  $\text{CoO}_2$  plane for the present value of  $D_2$ .

Consider now doping increasing further beyond  $x = \frac{2}{9}$ . One finds then an interesting evolution of polaronic structures which self-organize. High-spin states arise again and the number of ions with  $S \simeq \frac{5}{2}$  spins is equal to the number of doped holes, while low

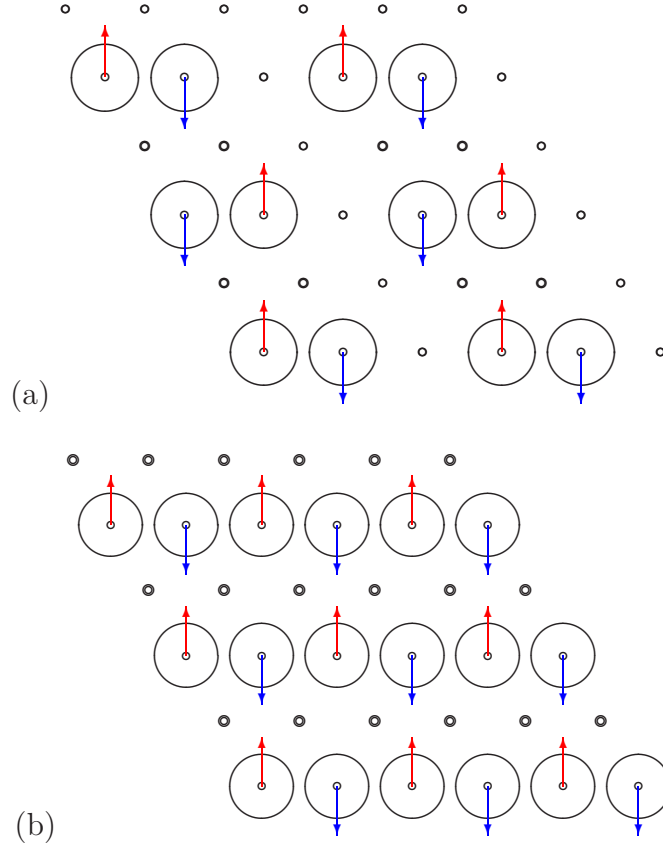


**Figure 4.** Stripe-like structures of high spin doped holes (spin values at sites with high hole density (circles) are very close to  $S = \frac{5}{2}$ ) in ground states for dopings: (a)  $x = \frac{1}{3}$  (upper panel) and (b)  $x = \frac{1}{2}$  (lower panel). Dots correspond to lattice sites, arrows indicate high spin states and each circle corresponds to  $\sim 0.8e$  hole charge. Parameters as in equation (13) and:  $B = 0.1 \text{ eV}$ ,  $D_2 = 1.25 \text{ eV}$ ,  $g_{\text{JT}} = 1.6 \text{ eV}\text{\AA}^{-1}$ ,  $K_{\text{JT}} = 13 \text{ eV}\text{\AA}^{-2}$ ,  $K_{\text{br}}/K_{\text{JT}} \gg 1$ . High HOMO-LUMO gaps indicate that the ground states are insulating.

spin and intermediate spin states are absent. There is a pronounced tendency to form first hole pairs with singlet-like spin states and to place such singlets maximizing the distance one from another. At doping of  $x = \frac{1}{3}$  pairs of polarons are ordered indeed in a pattern which maximizes their distances from one another, see figure 4(a). At half-doped system ( $x = \frac{1}{2}$ ) the lines of polarons form instead and the spin order along each line is AF, see figure 4(b). This result corroborates with the insulating character of both states which makes superexchange between pairs of  $\text{Co}^{4+}$  ions at ions doped with holes the most important magnetic exchange process.

Finally, a highly doped regime  $\frac{1}{2} < x < 1$  is characterized by stripe-like ground states, with lines of weakly doped sites of (almost) nonmagnetic ions in between the ordered lines of polarons, see figures 5(a) and 5(b). Having the  $6 \times 6$  cluster size, we study the dopings where the number of holes  $n_h$  is divisible by 3. The holes occupy predominantly four lines in the considered clusters at  $x = \frac{4}{6}$  and  $x = \frac{5}{6}$ , and the sites doped by one hole to  $\text{Co}^{4+}$  ionic configurations have high spin  $S \simeq \frac{5}{2}$ . As the electron

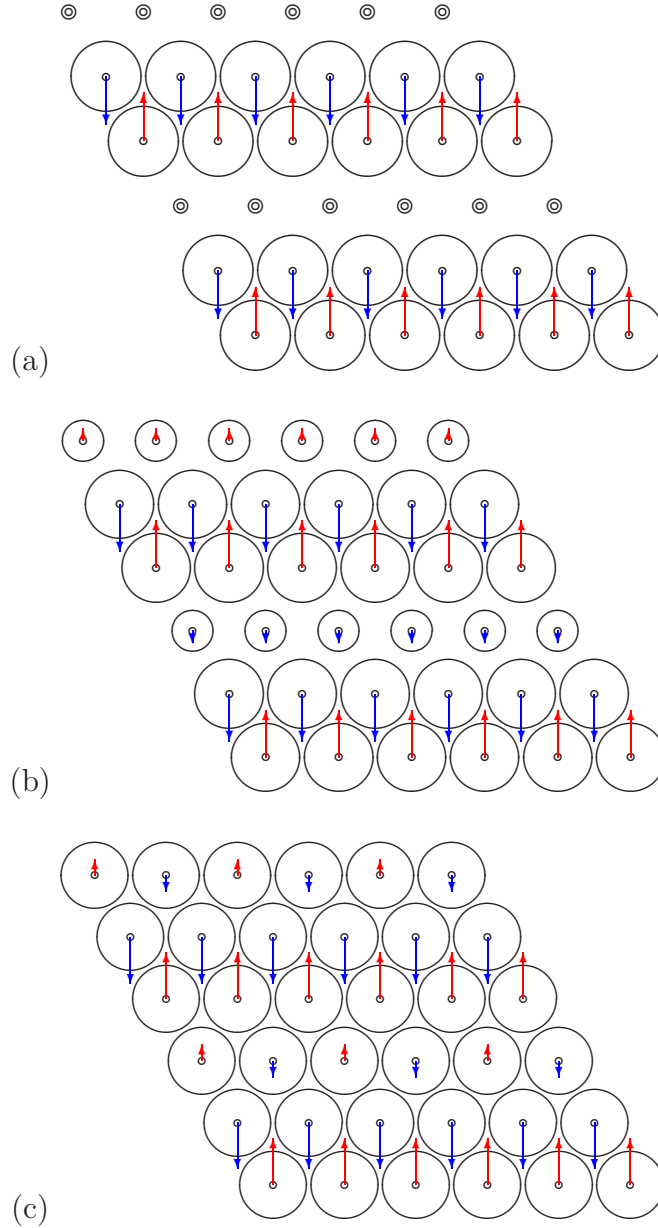


**Figure 5.** Thick stripe-like walls of high spin doped holes (spin values are very close to  $S = \frac{5}{2}$ ) in ground states obtained for doping: (a)  $x = \frac{4}{6}$  (upper panel), (b)  $x = \frac{5}{6}$  (middle panel), and (c)  $x = 1$  (lower panel). Parameters as in equation (13) and:  $B = 0.1$  eV,  $D_2 = 1.25$  eV,  $g_{\text{JT}} = 1.6$  eV $\text{\AA}^{-1}$ ,  $K_{\text{JT}} = 13$  eV $\text{\AA}^{-2}$ ,  $K_{\text{br}}/K_{\text{JT}} \gg 1$ . Hole charges are  $\sim 1e$  at high spin sites, while smaller circles correspond to  $\sim 0.6e$  charge. Low spin states are found at higher doping: (b)  $S \sim \frac{1}{4}$ , and (c)  $S \sim \frac{1}{2}$ . Relatively high HOMO-LUMO gaps indicate that the ground states are insulating.

density is there somewhat higher than 5 electrons per site, the magnetic moments order along the lines to the FM state which reflects weak double exchange mechanism [48] in cobaltates. For other dopings (not shown) this high symmetry of the solutions is lifted — however, the same trends (as visible in figures 3, 4 and 5) to form symmetric ground states for “magic dopings” is still clearly visible.

It is remarkable that such stripe-like structure survives even in the limit of  $x = 1$ , see figure 5(c), and was obtained from unbiased initial configurations as the most stable state. Surprisingly, the lines which separate the ordered structure of high spin polarons have here low spins  $S \simeq \frac{1}{2}$ , and these spins have AF order along their lines, in contrast to the FM order along lines of large  $S \simeq \frac{5}{2}$  spins. Such a state may be understood as following from weak AF superexchange which becomes active when one  $t_{2g}$  hole couples the neighbouring low spin ions. At the same time, absence of high spins at every third line reduces frustration of magnetic interactions.

## 5. Discussion and Summary

The results we obtained for increasing doping in  $\text{CoO}_2$  planes are somewhat unexpected. A systematic trend was found that doping creates high spin ( $S = \frac{5}{2}$ ) states and holes are pretty well localized on  $\text{Co}^{4+}$  ions. Note that orbital degrees of freedom are saturated here (for  $S = \frac{5}{2}$  states) so Jahn-Teller distortions or spin-orbital entanglement are not expected. So far, there is no clear and direct experimental support for such hole localization in form of high spin ( $S = \frac{5}{2}$ ) states, and they were not reported in doped Na-compounds. The only exception is found in layered  $\text{Li}_{1-x}\text{CoO}_2$  for very low doping level  $0 < x < 0.06$  [49]. Also for  $x = 0.5$  neutron scattering study of  $\text{Na}_{0.5}\text{CoO}_2$  gives the charge and spin order in agreement with that shown in figure 4(b), but the authors [50] interpret their data in terms of low  $S = \frac{1}{2}$  spins. For lower Na concentration  $1 - x \sim 0.3$  there is some evidence of antiferromagnetic spin-spin correlations [51].

The central result concerning the electronic structure, is that all the investigated ground states are insulating (sizable HOMO-LUMO gaps). On the contrary, it is well known that the ground state of  $\text{Na}_{0.75}\text{CoO}_2$  is metallic [52]. Other systems where high spins [26, 27] or stripe structures [53] were found are clearly beyond the assumptions made within the present model (due to several reasons; to give one simple example, due to the presence of  $\text{Co}^{2+}$  ions). This in our opinion does not invalidate the results we obtained upon assumption that the system is a truly regular 2D triangular plane. Namely, the experimental data [54] on  $\text{Na}_{1-x}\text{CoO}_2$  and subsequent theoretical investigation [15, 55] clearly show that the assumption made about 2D uncoupled layers in  $\text{Na}_x\text{CoO}_2$  is an idealization that does not reflect the properties of real systems. Only for smaller content of Na ions (higher doping  $x$ ) the 2D nature of electrons in  $\text{Na}_{1-x}\text{CoO}_2$  is enhanced (and the antiferromagnetic spin correlation increases) [56]. Thus, there is a significant 3D component to the real layered system and therefore 2D computations are expected to show rather different charge and magnetization distribution from the experimental data.

At present, our results can be treated as a prediction pending until some new truly 2D system with a triangular lattice is discovered and investigated. Also for the already discussed systems with low hole concentration  $x$  one might expect that entangled spin states with up and down high spin pairs would form. Observation of such entangled states in real systems, their treatment in the theory, and search for intermediate spin ( $S = 1$ )

states which could be stabilized by quantum effects beyond the present theory [32], provide experimental challenges in the physics of cobalt oxides.

Summarizing, we have established a generic trend that doping of  $\text{CoO}_2$  planes induces localized hole states with high  $S = \frac{5}{2}$  spins. This releasing of spin states at the doped  $\text{Co}^{4+}$  ions with reduced electron density and partly filled  $e_g$  orbitals makes it necessary to consider the full five-band model including  $\text{Co}(3d)$  orbitals [8], in spite of having (almost) empty  $e_g$  orbitals in undoped compounds with a higher electron density. The present study suggests as well that one has to use then the full Hund's exchange tensor for a realistic description. The doped holes first *self-organize* into polaronic states consisting of two holes each in the regime of low doping, and next form ordered 1D structures when doping approaches  $x = \frac{1}{3}$ . We suggest that superexchange between  $S = \frac{5}{2}$  spins is the dominating magnetic interaction which is responsible for the antiferromagnetic spin order along the 1D lines up to half-doping ( $x = \frac{1}{2}$ ). Higher doping generates triangles occupied by three spins  $S = \frac{5}{2}$  spins and superexchange interactions are frustrated. In this regime the system selects antiferromagnetic order with lines of ferromagnetic spins which are believed to follow from weak FM double exchange mechanism [48]. Surprisingly, low spin  $S = \frac{1}{2}$  states survive *even* in the fully doped case ( $x = 1$ ) and serve to stabilize the magnetic order of large spins along the AF 1D structures with pairs of lines containing ferromagnetic spins each. One could expect however that such an ordered phase will be destabilized by quantum fluctuations and a disordered magnetic state would arise instead.

As a final remark let us address the question of possible future extensions of this model approach: Are possible changes of the Hamiltonian parameters not needed to describe  $\text{Na}_{1-x}\text{CoO}_2$  and how robust the results might be with respect to them? It would be indeed quite interesting to repeat all the computations for different sets of the Hamiltonian parameters. However, as mentioned above, such computations are very time consuming so further numerical studies could be motivated only by experimental information concerning more precise values of the parameters for the systems with  $\text{CoO}_2$  planes. We expect that this information will become available due to future experiments.

## Acknowledgments

We kindly acknowledge financial support by the Polish National Science Center (NCN) under Project No. 2012/04/A/ST3/00331.

## Appendix: Hopping elements in the effective model

Here we present supplementary data which justify the choice of hopping parameters and give more details on the values of hopping elements which are used in the kinetic energy (2) in the effective model for  $3d$  electrons (1) in section 2, see tables 1 and 2. We begin with the hopping elements resulting from indirect Co-O-Co hopping, and next present direct Co-Co hopping. These two different sets of hopping elements are given by two



**Table 1.** Effective hopping elements  $t_{i\mu,j\nu}$  between orbitals  $\mu$  and  $\nu$  at sites  $i$  and  $j$  resulting from indirect cobalt-oxygen-cobalt transitions in a triangular lattice as obtained using Slater-Koster rules [16] and perturbation theory [17], in units of  $t_0 = P_{pd\pi}^2/\Delta$ . Bond directions are given by lattice vectors  $\mathbf{a}_n$ , see equation (3). Furthermore, we use the ratio  $P_{pd\sigma}/P_{pd\pi} = -2.0$  [10, 34, 35]. The entries for  $\nu < \mu$  were omitted as symmetry implies that  $t_{i\mu,j\nu} = t_{i\nu,j\mu}$ .

$i$	$j$	$\mu$	$\nu$	$t_{i\mu,j\nu}$
0	$\mathbf{a}_1$	$xy$	$zx$	$t_0$
0	$\mathbf{a}_1$	$yz$	$3z^2 - r^2$	$-t_0$
0	$\mathbf{a}_1$	$yz$	$x^2 - y^2$	$\sqrt{3}t_0$
0	$\mathbf{a}_2$	$xy$	$yz$	$t_0$
0	$\mathbf{a}_2$	$zx$	$3z^2 - r^2$	$-t_0$
0	$\mathbf{a}_2$	$zx$	$x^2 - y^2$	$-\sqrt{3}t_0$
0	$\mathbf{a}_3$	$yz$	$zx$	$t_0$
0	$\mathbf{a}_3$	$xy$	$3z^2 - r^2$	$2t_0$

parameters,  $t_0$  and  $t_1$ , respectively.

The hybridization elements  $P_{pd\sigma}$  and  $P_{pd\pi}$  are the appropriate Slater-Koster interatomic integrals [16] and  $\Delta$  is charge-transfer energy between bare cobalt 3d level and oxygen 2p level [10, 13, 34]. The original estimates for  $P_{pd\sigma}$ ,  $\Delta$  and  $t_0$  are, respectively: 1.8 eV, 2.0 eV and 0.67 eV [34]; 2.5 eV, 2.0 eV and 0.35 eV [10]; 2.35 eV, 2.9 eV and 0.34 eV [12]; 2.3 eV, 1.0 eV (here an effective value of  $\Delta$  is given) and 1.1 eV [35]; 1.4 eV, 3.2 eV and 0.15 eV [23]. In general, the quoted values, if studied within multiband HF approaches, differ from those coming out when *ab initio* results are combined with (i.e., they are fitted to) particular experimental results. This large variation of parameters occurs because in the first group of papers the correlations are not included (they could be included only in an *a posteriori* HF treatment). On the contrary, in the second group of papers effective models are constructed for the description of particular experimental data and have the correlations included (within the effective Hamiltonian parameters) just from the beginning. On top of it effective models use the Hamiltonian parameters which come out from complicated renormalisation and/or superposition of various physical ingredients. The largest difference in the above mentioned two groups of papers can be expected for the values of  $\Delta$ . Finally, let us note that various *ab initio*-like evaluations and other direct estimates of  $t_0$  are:  $\sim 0.1$ - $0.3$  eV [40], 0.1 eV [9, 11, 21, 57] and (already mentioned) 0.15 eV [23]. Here we take  $t_0 = P_{pd\pi}^2/\Delta = 0.3$  eV.

In addition, the ratio  $P_{pd\sigma}/P_{pd\pi}$  has to be fixed. In a simplified approach  $P_{pd\sigma}/P_{pd\pi} = -\sqrt{3}$ , see [58]; other reported values are higher:  $P_{pd\sigma}/P_{pd\pi} = -2.16$  [10, 34, 35] and  $P_{pd\sigma}/P_{pd\pi} = -2.35$  [12]. Here we take  $P_{pd\sigma}/P_{pd\pi} = -2.0$  — just for the sake of simplicity. With this latter choice the entries in table 1 representing hopping elements for pairs of different orbitals at neighbouring Co ions are simpler while the qualitative results of this study do not change when a slightly different value of the

**Table 2.** The direct cobalt-cobalt hopping elements  $t_{i\mu,j\nu}$  between orbitals  $\mu$  and  $\nu$  at sites  $i$  and  $j$  for the triangular lattice, in units of  $t_1 \equiv \frac{1}{2}P_{dd\pi}$ , and with  $P_{dd\sigma}/P_{dd\pi} = -2.0$  [35]. The symmetry implies that entries for  $\nu < \mu$  are the same as those for  $\nu > \mu$ .

$i$	$j$	$\mu$	$\nu$	$t_{i\mu,j\nu}$
0	$\mathbf{a}_1$	$xy$	$xy$	$t_1$
0	$\mathbf{a}_1$	$xy$	$zx$	$-t_1$
0	$\mathbf{a}_1$	$yz$	$yz$	$-3t_1$
0	$\mathbf{a}_1$	$yz$	$x^2 - y^2$	$-\frac{3}{2}t_1$
0	$\mathbf{a}_1$	$yz$	$3z^2 - r^2$	$\frac{\sqrt{3}}{2}t_1$
0	$\mathbf{a}_1$	$zx$	$zx$	$t_1$
0	$\mathbf{a}_1$	$x^2 - y^2$	$x^2 - y^2$	$-\frac{1}{4}t_1$
0	$\mathbf{a}_1$	$x^2 - y^2$	$3z^2 - r^2$	$\frac{3\sqrt{3}}{4}t_1$
0	$\mathbf{a}_1$	$3z^2 - r^2$	$3z^2 - r^2$	$\frac{5}{4}t_1$
0	$\mathbf{a}_2$	$xy$	$xy$	$t_1$
0	$\mathbf{a}_2$	$xy$	$yz$	$-t_1$
0	$\mathbf{a}_2$	$yz$	$yz$	$t_1$
0	$\mathbf{a}_2$	$zx$	$zx$	$-3t_1$
0	$\mathbf{a}_2$	$zx$	$x^2 - y^2$	$\frac{3}{2}t_1$
0	$\mathbf{a}_2$	$zx$	$3z^2 - r^2$	$\frac{\sqrt{3}}{2}t_1$
0	$\mathbf{a}_2$	$x^2 - y^2$	$x^2 - y^2$	$-\frac{1}{4}t_1$
0	$\mathbf{a}_2$	$x^2 - y^2$	$3z^2 - r^2$	$-\frac{3\sqrt{3}}{4}t_1$
0	$\mathbf{a}_2$	$3z^2 - r^2$	$3z^2 - r^2$	$\frac{5}{4}t_1$
0	$\mathbf{a}_3$	$xy$	$xy$	$-3t_1$
0	$\mathbf{a}_3$	$xy$	$3z^2 - r^2$	$-\sqrt{3}t_1$
0	$\mathbf{a}_3$	$yz$	$yz$	$t_1$
0	$\mathbf{a}_3$	$yz$	$zx$	$-t_1$
0	$\mathbf{a}_3$	$zx$	$zx$	$t_1$
0	$\mathbf{a}_3$	$x^2 - y^2$	$x^2 - y^2$	$2t_1$
0	$\mathbf{a}_3$	$3z^2 - r^2$	$3z^2 - r^2$	$-t_1$

ratio  $P_{pd\sigma}/P_{pd\pi}$  is chosen.

Unfortunately, much less is known about direct cobalt-cobalt hopping elements — the majority of authors assume that they are negligible. Here we adopt the ratio  $P_{dd\sigma}/P_{dd\pi} = -2.0$  and take a value  $P_{dd\pi} = 0.1$  eV, following Bourgeois *et al* [11]. We also remark that according to Harrison rules  $P_{dd\sigma}/P_{dd\pi} = -1.5$  [58], but having so small direct  $d$ - $d$  hopping elements no qualitative changes of the results are expected when the above ratio would be taken instead. Complete list of direct cobalt-cobalt hopping elements for different pairs of orbitals at nearest neighbour Co ions is given in table 2.

## References

- [1] Imada M, Fujimori A and Tokura Y 1998 *Rev. Mod. Phys.* **70** 1039
- [2] Korotin M A, Eshov Yu A, Solovyev I V, Anisimov V I, Khomskii D I and Sawatzky G A 1996 *Phys. Rev. B* **54** 5309
- [3] Dagotto E, Hotta T and Moreo A 2001 *Phys. Rep.* **344** 1  
Dagotto E 2005 *New J. Phys.* **7** 67  
Weiße A and Fehske H 2004 *New J. Phys.* **6** 158
- [4] Kovaleva N N, Oleś A M, Balbashov A M, Maljuk A, Argyriou D N, Khaliullin G and Keimer B 2010 *Phys. Rev. B* **81** 235130
- [5] Feiner L F and Oleś A M 1999 *Phys. Rev. B* **59** 3295  
Oleś A M, Khaliullin G, Horsch P and Feiner L F 2005 *Phys. Rev. B* **72** 214431
- [6] Foo M L, Wang Y Y, Watauchi S, Zandbergen H W, He T, Cava R J and Ong N P 2004 *Phys. Rev. Lett.* **92** 247001
- [7] de Vaulx C, Julien M-H, Berthier C, Horvatić M, Bordet P, Simonet P V, Chen D P and Lin C T 2005 *Phys. Rev. Lett.* **95** 186405  
Lang C, Bobroff J, Alloul H, Mendels P, Blanchard N and Collin G 2005 *Phys. Rev. B* **72** 094404
- [8] Khaliullin G and Chaloupka J 2008 *Phys. Rev. B* **77** 104532
- [9] Bourgeois A, Aligia A A and Rozenberg M J 2009 *Phys. Rev. Lett.* **102** 066402
- [10] Mizokawa T 2004 *New Journal of Physics* **6** 169
- [11] Bourgeois A, Aligia A A, Kroll T and Núñez-Regueiro M D 2007 *Phys. Rev. B* **75** 174518
- [12] Kroll T, Aligia A A and Sawatzky G A 2006 *Phys. Rev. B* **74** 115124
- [13] Koshibae W and Maekawa S 2003 *Phys. Rev. Lett.* **91** 257003
- [14] Indergand M, Yamashita Y, Kusunose H and Sigrist M 2005 *Phys. Rev. B* **71** 214414
- [15] Yamakawa Y and Ono Y 2007 *J. Phys.: Condens. Matter* **19** 145289  
Yamakawa Y, Watanabe N and Ono Y 2010 *J. Phys.: Conf. Series* **200** 012233
- [16] Slater C and Koster G F 1954 *Phys. Rev.* **94** 1498  
Mehl M J *Slater-Koster Tight-Binding Matrix Elements*:  
<http://cst-www.nrl.navy.mil/users/mehl/sk-param.html>
- [17] Zaanen J and Oleś A M 1993 *Phys. Rev. B* **48** 7197
- [18] Toyozawa Y and Inoue M 1996 *J. Phys. Soc. Jpn.* **21** 1663
- [19] Rościszewski K and Oleś A M 2008 *J. Phys.: Condens. Matter* **20** 365212  
Rościszewski K and Oleś A M 2010 *J. Phys.: Condens. Matter* **22** 425601
- [20] Pradheesh R, Nair H S, Sankaranarayanan V and Sethupathi K 2012 *Eur. J. Phys. B* **85** 260
- [21] Kroll T 2006 *On the structure of layered sodium cobalt oxides*, Ph.D. thesis, Technischen Universität Dresden, Dresden
- [22] Pillay D, Johannes M D, Mazin I I and Andersen O K 2008 *Phys. Rev. B* **78** 012501
- [23] Zou L-J, Wang J L and Zeng Z 2004 *Phys. Rev. B* **69** 132505
- [24] Zaliznyak I A, Hall J P, Tramquada J M, Erwin R and Morimoto Y 2000 *Phys. Rev. Lett.* **85** 4353
- [25] Huang Q, Foo M L, Pascal R A Jr, Lynn J W, Toby B H, He T, Zandbergen H W and Cava R J 2004 *Phys. Rev. B* **70** 184110
- [26] Merz M, Fuchs D, Assmann A, Uebe S, v.Loehneysen H, Nagel P and Schuppler S 2011 *Phys. Rev. B* **84** 014436
- [27] Hollaman N, Haverkort M W, Cwik M, Benomer M, Reuther M, Tanaka A and Lorentz T 2008 *New J. Phys.* **10** 023018
- [28] Oleś A M 1983 *Phys. Rev. B* **28** 327
- [29] Horsch P 2007 *Orbital Physics in Transition-metal Oxides: Magnetism and Optics*, in Handbook of Magnetism and Advanced Magnetic Materials, edited by Kronmüller H and Parkin S 2007, Volume 1: *Fundamentals and Theory*, J. Wiley and Sons, Ltd.
- [30] Griffith J S 1971 *The Theory on Transition Metal Ions*, Cambridge University Press
- [31] Bünnemann J, Gebhard F, Ohn T, Weiser S and Weber W 2005 *Gutzwiller-Correlated Wave*

- Functions: Application to ferromagnetic nickel*, in the Chapter: Parameters for the Coulomb Interaction, arXiv.org, Cornell Univ. Library, arXiv:cond-mat/0503332.
- [32] Oleś A M 2012 *J. Phys.: Condens. Matter* **24** 313201
- [33] Horsch P and Oleś A M 2011 *Phys. Rev. B* **84** 064429  
Avella A, Horsch P and Oleś A M 2013 *Phys. Rev. B* **87** 045132
- [34] Mizokawa T and Fujimori A 1995 *Phys. Rev. B* **51** 12880  
Mizokawa T and Fujimori A 1996 *Phys. Rev. B* **54** 5368
- [35] Wakisaka Y, Hirata S, Mizokawa T, Suzuki Y, Miyazaki Y and Kajitani T 2008 *Phys. Rev. B* **78** 235107
- [36] Zhang W, X Huang Q, Zhang W and Hu A 2004 *J. Appl. Phys.* **95** 6822
- [37] Wu W B, Huang D J, Okamoto J, Tanaka A, Lin H J, Chou F C, Fujimori A and Chen C T 2005 *Phys. Rev. Lett.* **94** 146402
- [38] Lee K-W, Kuneš J and Pickett W E 2004 *Phys. Rev. B* **70** 045104
- [39] Tanaka A and Hu X 2003 *Phys. Rev. Lett.* **91** 257006
- [40] Landron S and Lepetit M 2006 *Phys. Rev. B* **74** 184507
- [41] Stollhoff G and Fulde P 1980 *J. Chem. Phys.* **73** 4548  
Stollhoff G 1996 *J. Chem. Phys.* **105** 227  
Fulde P 1991 *Electron Correlations in Molecules and Solids*, Springer Series in Solid State Sciences, Vol. 100, Springer Verlag, Berlin.
- [42] Oleś A M, Zaanen J and Fulde P 1987 *Physica B&C* **148** 260  
Oleś A M and Grzelka W 1991 *Phys. Rev. B* **70** 9531
- [43] Rościszewski K and Oleś A M 2011 *J. Phys.: Condens. Matter* **23** 265601
- [44] Oleś A M, Pfirsch F, Fulde P and Böhm M C 1986 *J. Chem. Phys.* **85** 5183  
Oleś A M, Pfirsch F, Fulde P and Böhm M C 1987 *Z. Phys. B* **66** 359
- [45] Seo H, Posadas A and Demkov A A 2012 *Phys. Rev. B* **86** 014430
- [46] Sboychakov A O, Kugel K I, Rakhmanov A L and Khomskii D I 2009 *Phys. Rev. B* **80** 024423
- [47] Zaanen J, Paxton A T, Sepsen O and Andersen O K 1988 *Phys. Rev. B* **60** 2685.
- [48] de Gennes P G 1960 *Phys. Rev. B* **118** 141  
van den Brink J and Khomskii D I 1999 *Phys. Rev. Lett.* **82** 1016  
Oleś A M and Feiner L F 2002 *Phys. Rev. B* **65** 052414  
Daghofer M, Oleś A M and von der Linden W 2004 *Phys. Rev. B* **70** 184430  
Oleś A M and Khaliullin G 2011 *Phys. Rev. B* **84** 214414
- [49] Hertz J T, Huang Q, McQueen T, Klimczuk T, Bos J W G, Viciu L and Cava R J 2008 *Phys. Rev. B* **77** 075119
- [50] Gasparovic G, Ott R A, Cho J H, Chou F C, Chu Y, Lynn J W and Lee Y S 2006 *Phys. Rev. Lett.* **96** 046403
- [51] Ohira-Kawamura S, Nagata T, Takeda K and Yoshizawa H 2010 *Physica C* **470** S691
- [52] Garbarino G, Monteverde M, Núñez-Regueiro M, Acha C, Foo M L and Cava R J 2008 *Phys. Rev. B* **77** 064105
- [53] Cwik M, Benomar M, Finger T, Sidis Y, Senff D, Reuther M, Lorenz T and Braden M 2009 *Phys. Rev. Lett.* **102** 057201
- [54] Yokoi M, Moyoshi T, Kobayashi Y, Soda M, Yasui Y, Sato M and Kakurai L 2005 *J. Phys. Soc. Jpn.* **74** 3046
- [55] Helme L M, Boothroyd A T, Coldea R, Prabakaran D, Stunault A, McIntyre G J and Kernavanois N 2006 *Phys. Rev. B* **73** 054405
- [56] Yokoi M, Moyoshi T, Kobayashi Y, Soda M, Yasui Y, Sato M and Kakurai K 2005 *J. Phys. Soc. Jpn.* **74** 3046
- [57] Khaliullin G, Koshibae W and Maekawa S 2004 *Phys. Rev. Lett.* **93** 176401
- [58] Harrison W A 2005 *Elementary Electronic Structure*, World Scientific, London